

Properties of discrete breathers in graphane from *ab initio* simulations

G.M. Chechin¹, S.V. Dmitriev^{2,3}, I.P. Lobzenko¹, D.S. Ryabov¹

¹ *Research Institute of Physics, Southern Federal University, 194 Stachki Av, Rostov-on-Don 344090, Russia*

² *Institute for Metals Superplasticity Problems of RAS, 39 Khalturin St, Ufa 450001, Russia and*

³ *National Research Tomsk State University, 36 Lenin Prospekt, Tomsk 634050, Russia*

(Dated: September 28, 2018)

A density functional theory (DFT) study of the discrete breathers (DBs) in graphane (fully hydrogenated graphene) was performed. To the best of our knowledge, this is the first demonstration of the existence of DBs in a crystalline body from the first-principle simulations. It is found that the DB is a robust, highly localized vibrational mode with one hydrogen atom oscillating with a large amplitude along the direction normal to the graphane plane with all neighboring atoms having much smaller vibration amplitudes. DB frequency decreases with increase in its amplitude, and it can take any value within the phonon gap and can even enter the low-frequency phonon band. The concept of DB is then used to propose an explanation to the recent experimental results on the nontrivial kinetics of graphane dehydrogenation at elevated temperatures.

PACS numbers: 63.20.Pw, 63.20.Ry, 63.20.dk, 63.22.Rc, 88.30.R-

I. INTRODUCTION

Discrete breathers (DBs), also termed as intrinsic localized modes, are spatially localized, large-amplitude vibrational modes in defect-free nonlinear lattices. They have been identified as exact solutions to a number of model nonlinear systems possessing translational symmetry [1]. DBs were successfully observed experimentally in various physical systems such as two-dimensional array of optical waveguides [2]; Bose-Einstein condensate [3]; one-dimensional micromechanical array of coupled cantilevers [4]; two-dimensional nonlinear electrical lattices [5]; underdamped Josephson-junction array [6]; quasi-one-dimensional biaxial antiferromagnet [7] and others.

Diversity of physical systems supporting DBs suggests that they are very common in nonlinear lattices. Crystals are natural nonlinear lattices and many studies, both experimental [8–11] and numerical [12–17, 19], have been done to prove the existence of DBs and to use them for explanation of various physical effects in crystals [10, 21–25]. Let us mention the detection of DBs from the resonant Raman scattering measurements in a complex compound termed as PtCl [8]; from inelastic x-ray and neutron scattering data in α -uranium [10]; from inelastic neutron scattering spectra in NaI [11]. It should be noted that experimental observation of DBs in crystals is a challenge because their contribution to the vibrational density of states is masked by the contribution from thermal lattice vibrations [26]. In these circumstances the importance of numerical studies cannot be overestimated. Molecular dynamics based on empirical interatomic potentials was used to identify DBs (or, more precisely, quasi-breathers [27]) in NaI [12], in Si and Ge [13], in Ni and Nb [14], in C₆₀ fullerite nanocrystals [15]; in carbon nanotubes [16], graphene [17, 18] and graphane [19]. In the work [20] a group-theoretical approach has been developed to simplify the analysis of existence and

stability of DBs of different symmetry types in nonlinear lattices. The approach can also be applied to the analysis of DBs in two-dimensional structures such as graphene and graphane.

Molecular dynamics studies rely on the quality of interatomic potentials, which is always a question. For instance, the authors of the work [13] report that they have tried different interatomic potentials to model DBs in Si and have succeeded only with the Tersoff potential. The reason is that the interatomic potentials are often fitted to the elastic moduli and phonon spectra of crystals (calculated from linearized equations of motion) as well as to some experimentally measurable energies, such as the sublimation energy, vacancy energy, etc. (for which not the exact profile of the potential functions but their integral characteristics are important since the change in potential energy is path independent). On the other hand, DB, being an essentially nonlinear vibrational mode, is sensitive to the exact shape of the potentials. In this study it will be demonstrated that the molecular dynamics simulation of DBs in graphane [19], performed using the LAMMPS package [29] with the AIREBO potential [30], gives an adequate estimation of DB frequency only for small amplitudes and shows a dramatic error for large amplitudes. At the same time, the AIREBO potential has been successfully used in a countless number of studies of various properties of hydrocarbon systems, meaning that indeed DBs provide a very severe test of the interatomic potentials.

Breather oscillations induce polarization of the outer electron shells of atoms, which is very difficult to fully capture in frame of the model considering interaction between mass points. There exist several works where polarization of electron shells induced by breather oscillations is partly taken into account. As an example, we refer to the works [21] where a simplified model was used to discuss the effect of polarization induced by DBs in

the perovskite structure.

The above discussion suggests the importance of *ab initio* simulations of DBs in crystals. So far, to the best of our knowledge, no such studies have been undertaken, possibly, because the application of DFT theory to dynamical problems is computationally costly. In this sense, graphane [31, 32] is a very good choice for the study because the highly localized DBs in a two-dimensional crystal can be analyzed using a computational cell with a small number of atoms. Furthermore, graphane is a new material promising for many applications [33]. Particularly, graphane holds a potential for hydrogen storage due to its lightweight structure and high performance [32–35]. It was shown that graphane can easily absorb hydrogen at low temperatures and desorb at high temperatures [32, 36, 37].

Dehydrogenation kinetics during annealing of graphane turns out to be not as simple as expected. It was found that there are two types of dehydrogenation mechanisms with different dehydrogenation barriers [37]. It is challenging to find a theoretical explanation of this effect.

Our motivation in this study is to legitimize the existence of discrete breathers in crystalline solids by means of DFT simulations using graphane as an example. We also aim to offer an explanation of the dehydrogenation kinetics of graphane at elevated temperatures.

The rest of the paper is organized as follows. In Sec. II the simulation details are briefly presented, then the results of DFT simulations are discussed in Sec. III. The results are discussed in Sec. IV and summarized in Sec. V.

II. SIMULATION DETAILS

In the present work, DB in graphane is studied with the aid of *ab initio* calculations. We use the ABINIT software package [38] implementing the methods of the density functional theory [39] (the corresponding algorithms can be found in [40]). The above package allows one to study dynamics of molecules and crystals in the framework of the Born-Oppenheimer approximation, which takes into account the significant differences in the masses of the atom nuclei and electrons [41]. The motion of heavy nuclei (ions) is described by the classical equations, while that of light electrons is controlled by the quantum mechanics equations. The forces acting on the nuclei depend on the electronic subsystem state, which quickly adapts to the nuclei current positions. Kohn-Sham equations [39] are solved by ABINIT for each nuclei configuration. Our calculations were performed based on the local density approximation and Troullier-Martins pseudopotentials. Plane waves are used as a basis set (with kinetic energy cutoff 40H) for the decomposition of electron eigenstates.

The chair confirmation of graphane [31] is considered with H atoms attached at the opposite sides of the graphane sheet, as shown in Fig. 1(a). Open (filled) dots

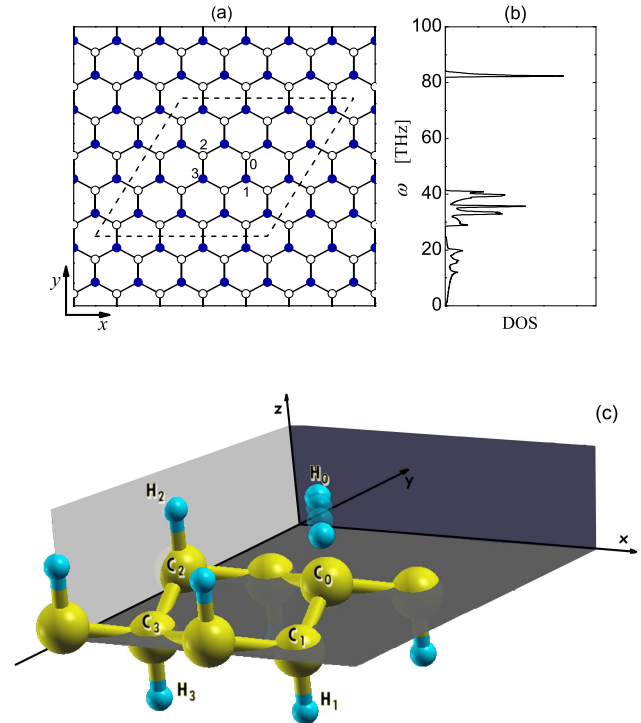


FIG. 1: (Color online) (a) Structure of graphane (CH). Open (filled) dots show carbon atoms with hydrogen atoms attached above (below) the sheet. The computational cell subjected to periodic boundary conditions is shown by the dashed line. To excite a DB, the H atom in the position 0, labeled as H_0 , was displaced along z axis (normal to the graphane sheet) and released with zero initial velocity. All other atoms had zero initial displacements and velocities. (b) Phonon density of states (DOS) of graphane. (c) Schematic presentation of the DB in graphane. The H_0 atom vibrates with a large amplitude while all other atoms have much smaller vibration amplitudes.

show carbon atoms with hydrogen atoms attached above (below) the sheet. The computational cell, shown by the dashed line, includes 32 carbon and 32 hydrogen atoms. Periodic boundary conditions are applied to exclude the effect of free edges.

III. SIMULATION RESULTS

Using the ABINIT package we have obtained the equilibrium structure of graphane with the C-C bond length equal to 1.520 Å, and the C-H bond length equal to 1.117 Å. Note that these parameters coincide with those reported in [31]. Due to the interaction with hydrogen atoms, the carbon atoms split into two sub-lattices with the off-plane displacements of ± 0.228 Å.

The calculated phonon density of states (DOS) for graphane is shown in Fig. 1(b). The center of the narrow

optical band is at a frequency of about 83 THz, while the width of this band is about 2 THz. The gap in the phonon spectrum extends from $\omega_L = 41.7$ THz to $\omega_H = 81.6$ THz having the width of 39.9 THz. These figures can be compared to the molecular dynamics results of the work [19] where the phonon gap edges were found to be 56.92 THz and 87.83 THz. Thus, the phonon gap we found is about 20% wider as compared to that given in Ref. [19]. Overall, the linear vibration spectrum reported in [19] is in a reasonable agreement with the *ab initio* results of the present study.

Existence of a wide gap in the phonon spectrum of graphene opens the possibility to excite a gap DB. This was achieved by applying a displacement normal to the graphene plane (along z axis) to the H atom in the position 0, labeled as H_0 [see Fig. 1(a)]. All other atoms in the computational cell had zero initial displacements and zero initial velocities. Varying the initial displacement of H_0 atom, DBs with different vibration amplitudes were excited. Figure 1(c) gives a schematic presentation of the DB in graphene. The H_0 atom vibrates with a large amplitude while all other atoms have much smaller vibration amplitudes.

In Fig. 2 the Δz displacements of the central atoms of DB, H_0 and C_0 (left panels), as well as Δz displacements of their nearest neighbors, H_1 and C_1 (right panels), are shown as the functions of time. Black (red) lines show the displacements of C (H) atoms. It can be seen that the H_0 atom shows large-amplitude, quasi-periodic oscillations. The C_0 atom vibrates with one order of magnitude smaller amplitude because carbon is 12 times heavier than hydrogen. Excited DBs are highly localized since the vibration amplitudes of the atoms H_1 and C_1 (and other atoms of the computational cell) are more than one order of magnitude smaller than that of H_0 atom.

In order to quantify the DB amplitude and frequency the $\Delta z(t)$ curve for H_0 atom is analyzed. The coordinates of the successive minimum and maximum points on the curve, $\Delta z_{\min}^{(n)}$, $t_{\min}^{(n)}$, $\Delta z_{\max}^{(n)}$, $t_{\max}^{(n)}$, numbered by the index n are determined. The amplitude and the oscillation period for the n -th half oscillation are defined as

$$\begin{aligned} A^{(n)} &= (\Delta z_{\max}^{(n)} - \Delta z_{\min}^{(n)})/2, \\ \omega_{\text{DB}}^{(n)} &= (2|t_{\max}^{(n)} - t_{\min}^{(n)}|)^{-1}, \end{aligned} \quad (1)$$

respectively. The quantities $A^{(n)}$ and $\omega_{\text{DB}}^{(n)}$ averaged over a few tens of periods are taken as A and ω_{DB} .

In Fig. 3 the DB frequency as the function of amplitude, $\omega_{\text{DB}}(A)$, is given. Edges of the phonon DOS gap are shown by the horizontal dashed lines. Dots labeled as a, b, and c (colored in red) correspond to the DBs presented in Fig. 2 (a,a'), (b,b'), and (c,c'), respectively. It can be seen that the $\omega_{\text{DB}}(A)$ curve bifurcates from the upper edge of the phonon gap and then decreases almost linearly with increase in A , entering the lower phonon band. The decrease in frequency with increase in amplitude reveals a soft-type anharmonicity of the DBs in graphene in the entire range of DB amplitudes.

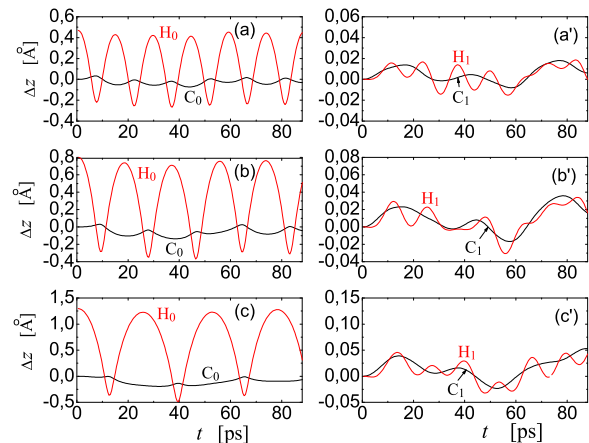


FIG. 2: (Color online) Displacements of atoms in the direction normal to the graphene plane as the functions of time. C_0 , H_0 are the central atoms of DB and C_1 , H_1 are their nearest neighbors [see Fig. 1(a)]. Black (red) lines show the displacements of C (H) atoms. Note different scale of ordinates used for the left and right panels. Amplitudes and frequencies of DBs are (a,a') $A = 0.34$ Å, $\omega_{\text{DB}} = 68.15$ THz; (b,b') $A = 0.54$ Å, $\omega_{\text{DB}} = 54.16$ THz; (c,c') $A = 0.82$ Å, $\omega_{\text{DB}} = 39.00$ THz.

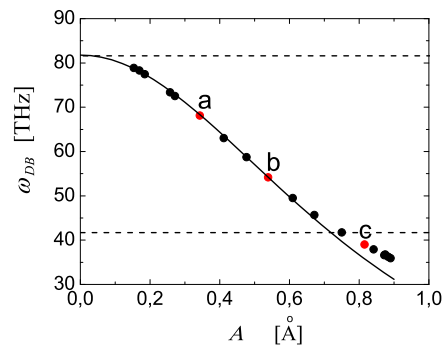


FIG. 3: (Color online) DB frequency as the function of amplitude from DFT simulation (scattered data). Solid line gives the analytical solution Eq. (4) for a point mass in the Morse potential. Horizontal dashed lines show the edges of gap in the phonon density of states, ω_L and ω_H . Dots labeled as a, b, and c (colored in red) correspond to the DBs presented in Fig. 2 (a,a'), (b,b'), and (c,c'), respectively.

In Fig. 4 the electron density distribution is shown in the vicinity of the DB for the case presented in Fig. 2 (a,a') and also marked by the red dot labeled as "a" in Fig. 3. Panels (a-c) of Fig. 4 correspond to the maximal, equilibrium and minimal distance between the C_0 and H_0 atoms constituting DB. Three sections by the (x, y) , (x, z) and (y, z) planes are shown. Within the pre-

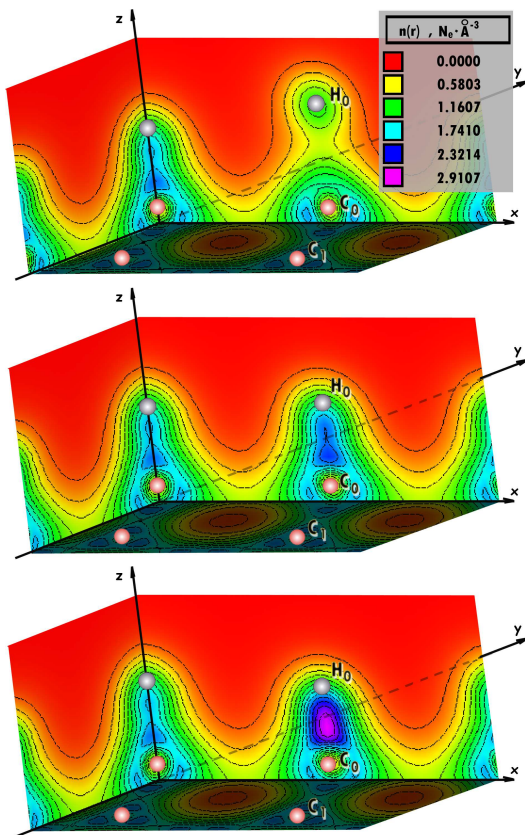


FIG. 4: (Color online) Electron density distribution in the vicinity of the DB for (a) maximal, (b) equilibrium and (c) minimal distance between the C_0 and H_0 atoms constituting DB. The case shown in Fig. 2 (a,a') (also marked by the red dot "a" in Fig. 3) is presented.

sented fragment the C_0 , C_1 , C_2 , C_3 , H_0 and H_2 atoms can be seen (see Fig. 1). It can be seen that due to the high degree of localization of the considered vibrational mode, the change in the C_0 - H_0 bond length results in a noticeable change in the electron density between these two atoms while it has marginal effect on the electron density of other regions, for instance, the C_0 - C_1 and C_2 - H_2 bond structures are practically same in the panels (a) to (c).

IV. DISCUSSION

Results of the present study can be compared to that in the molecular dynamics study [19] where the $\omega_{DB}(A)$ curve was predicted to decrease for small A , to increase for moderate A and again to decrease at large A . Such a non-monotonous $\omega_{DB}(A)$ curve with DB frequency above the phonon spectrum for large DB amplitudes is in a striking difference with our *ab initio* result presented in Fig. 3.

According to the conventional definition, stationary

DB is a time-periodic dynamical object [1]. Excitation of a DB in mathematical modeling requires the use of very refined initial conditions [43–45]. In the present study a simple method was used for DB excitation and this is why the DBs presented in Fig. 2 are not exactly time-periodic. The inaccuracy in the initial conditions results in radiation of a part of energy given to the system at $t = 0$ in the form of small-amplitude lattice vibrations that disturb the dynamics of DB. Spatially localized modes in nonlinear lattices that do not show exact periodicity in time can be interpreted as quasi-breathers [27].

It is well-known that a stable DB should not have frequency within the phonon spectrum of the crystal, otherwise it will excite the extended normal modes and gradually lose its energy. Therefore, the existence of the long-lived DBs with frequencies below ω_L , presented in Fig. 2 (c,c'), may look puzzling. The explanation is related to the fact that graphane has rigidity with respect to in-plane deformation much higher than bending rigidity. H_0 atom vibrating with a large amplitude exerts a force normal to the graphane sheet producing primarily bending deformation of the sheet. The bending phonon modes, due to small bending rigidity, have frequencies much lower than ω_L and thus they are barely excited by the DB with frequency just below ω_L . Similar arguments were used to explain the existence of long-lived DBs and DB clusters in strained graphane, having frequencies within the phonon band [17, 18].

Let us attempt to reproduce the $\omega_{DB}(A)$ dependence obtained for the DB in graphane (see Fig. 3) using the simplest one degree of freedom oscillator

$$m \frac{d^2 r}{dt^2} = - \frac{dU}{dr}, \quad (2)$$

where $m = 1.672 \times 10^{-27}$ kg is the hydrogen atom mass, $r(t)$ is the unknown coordinate of the atom as the function of time and

$$U(r) = D(1 - e^{-ar})^2 \quad (3)$$

is the Morse potential having minimum at $r = 0$, the bond energy D and stiffness a . Equation of motion (2) can be solved exactly, giving the following relation between frequency ω and amplitude $A = (r_{\max} - r_{\min})/2$

$$\omega = \frac{a}{\pi} \sqrt{\frac{D}{2m}} \operatorname{sech}(aA). \quad (4)$$

The solid curve (4) with the parameters $D = 4.28$ eV and $a = 1.80 \text{ \AA}^{-1}$ is plotted in Fig. 3. It can be seen that the scattered data obtained with the use of DFT simulations can be well fitted by the simple model in a wide range of A . Note that the value of D used for the fitting is in a perfect agreement with the C-H bond dissociation energy of 4.25 eV reported in [42].

We now turn to the discussion of recent experiments on thermally activated dehydrogenation of graphane [37]. Reportedly, there are two activation energies of dehydrogenation with the transition temperature at about

200°C. The smaller dehydrogenation activation energy at temperatures below 200°C can be understood by the metastable attachment of the energetic ions to the graphene sheet during plasma hydrogenation [36, 37]. However, the larger dehydrogenation activation energy at temperatures above 200°C has not yet been well explained. The nonlinear nature of the DBs implies that they do not appear at relatively small temperatures and instead are excited at higher temperatures. The fact that DBs can be externally excited at temperatures near 0K indicates that they can also be spontaneously excited at a finite-temperature thermal equilibrium [28, 46]. DBs spontaneously excited at finite temperatures may activate the dehydrogenation of hydrogenated graphene.

The following arguments have been recently developed to modify the reaction rate theory in solids taking into account DBs [22]. The classical expression for the reaction rate \dot{R} in thermal equilibrium reads

$$\dot{R} = R_0 \exp\left(-\frac{E}{k_B T}\right), \quad (5)$$

where R_0 is the frequency factor having dimension of inverse time, E is the reaction activation energy, $k_B = 8.617 \times 10^{-5} \text{ eVK}^{-1}$ is the Boltzmann constant, and T is temperature. In their theory it is assumed that due to the large-amplitude oscillations of atoms in the vicinity of DBs the activation energy (but not the temperature) is a (quasi)periodic function of time. For simplicity it is assumed that the height of the potential barrier is harmonically modulated, $E = E_0 + e \cos(\Omega t)$, with the amplitude e and frequency Ω . Even though the averaged over time potential barrier height is unchanged, the modulation results in the following correction of the escape rate [22]

$$\dot{R}(e) = \dot{R}I_0\left(\frac{e}{k_B T}\right), \quad (6)$$

where \dot{R} is the escape rate at $e = 0$ and I_0 is the zero-order modified Bessel function of the first kind. Note that $I_0(0) = 1$ and $I_0(x)$ is a rapidly growing function of x for $x > 0$. For example, for $e = 0.5 \text{ eV}$ at room temperature the reaction rate amplification factor is of order

of 10^7 , while for $T = 600 \text{ K}$ it is of order of 10^3 . This figures should be multiplied by the DB concentration which increases with increase in temperature according to the Arrhenius law [28, 46].

The above arguments suggest that DBs can considerably accelerate thermal fluctuation-activated chemical reactions such as dehydrogenation of graphane.

V. CONCLUSIONS

In conclusion, the existence of DBs in a crystal was demonstrated for the first time from *ab initio* calculations. Graphane was chosen for this study because it supports highly localized gap DBs, treatable by DFT simulations, and also because it is promising for a number of applications.

DBs in graphane demonstrate the soft-type anharmonicity with frequency monotonously decreasing with increasing amplitude. On the other hand, molecular dynamics simulations based on the AIREBO potential [19] give an adequate description of the $\omega_{\text{DB}}(A)$ curve only for small A and fail for large A . These results suggest that DBs provide a very severe test of the interatomic potentials used in molecular dynamics simulations.

The concept of DBs together with the reaction-rate theory that takes into account DBs were used to explain basic physics behind the dehydrogenation kinetics of graphane at finite temperatures.

Our work opens new direction for further research, which is analysis of properties of DBs in crystals by means of *ab initio* simulations.

The research was partly supported by the Russian Science Foundation (grant No14-13-00982) and by the Russian Foundation for Basic Research, grants 12-02-31507-mol-a and 14-02-97029-p-Povolzhie-a. The present results have been obtained through the use of the ABINIT code, a common project of the Université Catholique de Louvain, Corning Incorporated, and other contributors (URL <http://www.abinit.org>).

-
- [1] A.S. Dolgov, Sov. Phys. Solid State **28**, 907 (1986); A.J. Sievers, S. Takeno, Phys. Rev. Lett. **61**, 970 (1988); J.B. Page, Phys. Rev. B **41**, 7835 (1990); R.S. MacKay, S. Aubry, Nonlinearity **7**, 1623 (1994); S. Flach, C.R. Willis, Phys. Rep. **295**, 181 (1998); S. Flach, A.V. Gorbach, Phys. Rep. **467**, 1 (2008).
- [2] J.W. Fleischer, M. Segev, N.K. Efremidis, D.N. Christodoulides, Nature (London) **422**, 147 (2003).
- [3] A. Trombettoni, A. Smerzi, Phys. Rev. Lett. **86**, 2353 (2001); B. Eiermann, Th. Anker, M. Albiez, M. Taglieber, P. Treutlein, K.-P. Marzlin, M.K. Oberthaler, Phys. Rev. Lett. **92**, 230401 (2004).
- [4] M. Sato, S. Imai, N. Fujita, W. Shi, Y. Takao, Y. Sada, B.E. Hubbard, B. Ilic, A.J. Sievers, Phys. Rev. E **87**, 012920 (2013); M. Spletzer, A. Raman, A.Q. Wu, X. Xu, R. Reifenberger, Appl. Phys. Lett. **88**, 254102 (2006); J. Wiersig, S. Flach, K.H. Ahn, Appl. Phys. Lett. **93**, 222110 (2009).
- [5] L.Q. English, F. Palmero, P. Candiani, J. Cuevas, R. Carretero-Gonzalez, P.G. Kevrekidis, A.J. Sievers, Phys. Rev. Lett. **108**, 084101 (2012).
- [6] E. Trias, J.J. Mazo, T.P. Orlando, Phys. Rev. Lett. **84**, 741 (2000).
- [7] U.T. Schwarz, L.Q. English, A.J. Sievers, Phys. Rev.

- Lett. **83**, 223 (1999).
- [8] B.I. Swanson, J.A. Brozik, S.P. Love, G.F. Strouse, A.P. Shreve, A.R. Bishop, W.-Z. Wang, M.I. Salkola, Phys. Rev. Lett. **82**, 3288 (1999); N.K. Voulgarakis, G. Kalosakas, A.R. Bishop, G.P. Tsironis, Phys. Rev. B **64**, 020301 (2001); G. Kalosakas, A.R. Bishop, A.P. Shreve, Phys. Rev. B **66**, 094303 (2002).
- [9] D.K. Campbell, S. Flach, Y.S. Kivshar, Phys. Today **57**, 43 (2004).
- [10] M.E. Manley, A. Alatas, F. Trouw, B.M. Leu, J.W. Lynn, Y. Chen, W.L. Hulst, Phys. Rev. B **77**, 214305 (2008); M.E. Manley, M. Yethiraj, H. Sinn, H.M. Volz, A. Alatas, J.C. Lashley, W.L. Hulst, G.H. Lander, J.L. Smith, Phys. Rev. Lett. **96**, 125501 (2006).
- [11] M.E. Manley, A.J. Sievers, J.W. Lynn, S.A. Kiselev, N.I. Agladze, Y. Chen, A. Llobet, A. Alatas, Phys. Rev. B **79**, 134304 (2009); M. Kempa, P. Ondrejko, P. Bourges, J. Ollivier, S. Rols, J. Kulda, S. Margueron, J. Hlinka, J. Phys.: Condens. Matter **25**, 055403 (2013).
- [12] S.A. Kiselev, A.J. Sievers Phys. Rev. B **55**, 5755 (1997); L.Z. Khadeeva, S.V. Dmitriev, Phys. Rev. B **81**, 214306 (2010).
- [13] N.K. Voulgarakis, G. Hadjisavvas, P.C. Kelires, G.P. Tsironis, Phys. Rev. B **69**, 113201 (2004).
- [14] M. Haas, V. Hizhnyakov, A. Shelkan, M. Klopov, A.J. Sievers, Phys. Rev. B **84**, 144303 (2011).
- [15] A.V. Savin, Yu.S. Kivshar, Phys. Rev. B **85**, 125427 (2012).
- [16] T. Shimada, D. Shirasaki, T. Kitamura, Phys. Rev. B **81**, 035401 (2010).
- [17] J.A. Baimova, S.V. Dmitriev, K. Zhou, Europhys. Lett. **100**, 36005 (2012).
- [18] L.Z. Khadeeva, S.V. Dmitriev, Yu.S. Kivshar, JETP Lett. **94**, 539 (2011).
- [19] B. Liu, J.A. Baimova, S.V. Dmitriev, X. Wang, H. Zhu, K. Zhou, J. Phys. D: Appl. Phys. **46**, 305302 (2013).
- [20] G.S. Bezuglova, G.M. Chechin, P.P. Goncharov, Phys. Rev. E **84**, 036606 (2011).
- [21] A.R. Bishop, A. Bussmann-Holder, S. Kamba, M. Maglione, Phys. Rev. B **81**, 064106 (2010); J. Macutkevicius, J. Banys, A. Bussmann-Holder, A.R. Bishop, Phys. Rev. B **83**, 184301 (2011).
- [22] V.I. Dubinko, P.A. Selyshchev, J.F.R. Archilla, Phys. Rev. E **83**, 041124 (2011).
- [23] M.G. Velarde, J. Comput. Appl. Math. **233**, 1432 (2010).
- [24] A. Glensk, B. Grabowski, T. Hickel, and J. Neugebauer, Phys. Rev. X **4**, 011018 (2014).
- [25] J.F.R. Archilla, S.M.M. Coelho, F.D. Aurret, V.I. Dubinko, V. Hizhnyakov, arXiv:1311.4269 [cond-mat.mtrlsci] (2013).
- [26] A.J. Sievers, M. Sato, J.B. Page, T. Rössler, Phys. Rev. B **88**, 104305 (2013).
- [27] G.M. Chechin, G.S. Dzhelauhova, E.A. Mehonoshina, Phys. Rev. E **74**, 036608 (2006).
- [28] L.Z. Khadeeva, S.V. Dmitriev, Phys. Rev. B **84**, 144304 (2011).
- [29] S. Plimpton, J. Comput. Phys. **117** 1 (1995).
- [30] S.J. Stuart, A.B. Tutein, J.A. Harrison, J. Chem. Phys. **112** 6472 (2000).
- [31] M.H.F. Sluiter, Y. Kawazoe, Phys. Rev. B **68**, 085410 (2003); J.O. Sofo, A.S. Chaudhari, G.D. Barber, Phys. Rev. B **75**, 153401 (2007).
- [32] D.C. Elias, R.R. Nair, T.M. Mohiuddin, S.V. Morozov, P. Blake, M.P. Halsall, A.C. Ferrari, D.W. Boukhvalov, M.I. Katsnelson, A.K. Geim, K.S. Novoselov, Science **323**, 610 (2009).
- [33] C. Zhou, S. Chen, J. Lou, J. Wang, Q. Yang, C. Liu, D. Huang, T. Zhu, Nanoscale Res. Lett. **9**, 26 (2014).
- [34] R. Strobel, L. Jorissen, T. Schliermann, V. Trapp, W. Schutz, K. Bohmhammel, G. Wolf, J. Garcke, J. Power Sources **84**, 221 (1999).
- [35] W.C. Xu, K. Takahashi, Y. Matsuo, Y. Hattori, M. Kumagai, S. Ishiyama, K. Kaneko, S. Iijima, Int. J. Hydrogen Energy **32**, 2504 (2007).
- [36] M. Wojtaszek, N. Tombros, A. Caretta, P.H.M. Van Loosdrecht, B.J. Van Wees, J. Appl. Phys. **110**, 063715 (2011).
- [37] Z.Q. Luo, T. Yu, K.L. Kim, Z.H. Ni, Y.M. You, S. Lim, Z.X. Shen, S.Z. Wang, J.Y. Lin, ACS Nano **3**, 1781 (2009).
- [38] X. Gonze *et al.*, Comput. Phys. Commun. **180**, 2582 (2009).
- [39] P. Hohenberg, W. Kohn, Phys. Rev. **136**, B864 (1964); W. Kohn, L.J. Sham, Phys. Rev. **140**, A1133 (1965).
- [40] M.C. Payne, M.P. Teter, D.C. Allan, T.A. Arias, J.D. Joannopoulos, Rev. Mod. Phys. **64**, 1045 (1992).
- [41] D.R. Hamann, M. Schluter, C. Chiang, Phys. Rev. Lett. **43**, 1494 (1979). N. Troullier, J.L. Martins, Phys. Rev. B **43**, 1993 (1991).
- [42] S.J. Blanksby, G.B. Ellison, Accounts Chem. Res. **36** 255 (2003).
- [43] J.L. Marin, S. Aubry, Nonlinearity, **9**, 1501 (1998).
- [44] S. Flach, Computational studies of discrete breathers. In Energy Localization and Transfer (Eds. T. Dauxois et al., World Scientific, 2004), pp. 1-71.
- [45] G.M. Chechin, G.S. Bezuglova, J. Sound Vib. **322**, 490 (2009).
- [46] M.V. Ivanchenko, O.I. Kanakov, V.D. Shalfeev, S. Flach, Physica D **198** 120 (2004).